

# Anisotropic magnetoresistance contribution to measured domain wall resistances of in-plane magnetised (Ga,Mn)As

H.G. Roberts, S. Crampin, and S. J. Bending

Department of Physics, University of Bath, Bath BA2 7AY, UK

(Dated: November 19, 2018)

We demonstrate the presence of an important anisotropic magnetoresistance contribution to the domain wall resistance recently measured in thin-film (Ga,Mn)As with in-plane magnetic anisotropy. Analytic results for simple domain wall orientations supplemented by numerical results for more general cases show this previously omitted contribution can largely explain the observed negative resistance.

PACS numbers: 73.61.-r, 75.60.Ch, 75.50.Pp, 85.75.-d

The electrical resistance associated with current flow across a domain wall (DW) separating uniformly magnetised regions in a magnetic material has been the subject of investigation since the 1930s. A large volume of often contradictory results exists, mostly attributable to the difficulty in separating normally small intrinsic effects from the myriad of extrinsic effects that also contribute in magnetoresistance measurements.<sup>1</sup> In recent years some consensus has emerged in the study of DWs in metallic epitaxial films and nanostructures<sup>2</sup> where it is possible to more fully characterise and control the magnetic microstructure, with many results consistent with the spin-mistacking models of DW resistance.<sup>3,4</sup> Although the small magnitude of the DW resistance limits potential applications, significant enhancements at nanoconstrictions<sup>5</sup> allied with advances in the atomic-scale control of materials, raise hopes of practical magnetoresistive devices, whilst a close relationship with the phenomenon of current-induced DW motion<sup>6,7</sup> also makes the understanding of DW resistance of considerable importance.

It has been noted that enhanced magnetoresistance effects may be associated with DWs in ferromagnetic semiconductors due to the longer Fermi wavelength<sup>6</sup> and large exchange splitting relative to band width.<sup>8</sup> Rüster *et al.*<sup>9</sup> have observed an 8% increase in the magnetoresistance due to DWs pinned at < 10 nm constrictions in in-plane magnetised (Ga,Mn)As nanostructures, and Chiba *et al.*<sup>10</sup> report a significant positive DW magnetoresistance in perpendicularly magnetised (Ga,Mn)As layers consistent with the theory of Levy and Zhang.<sup>4</sup> Tang *et al.*<sup>11</sup> have studied the resistance of 30 – 100  $\mu\text{m}$  devices patterned from in-plane magnetised (Ga,Mn)As epilayers. By measuring the average resistance  $\langle R \rangle$  along the sides of the device channel as a 90° domain wall is driven through by current pulses, they find a small resistance drop. Scaling by a wall width of 10 nm, Tang *et al.* deduce a DW resistivity as large as  $\Delta\varrho/\rho \sim -100\%$  — a remarkable result implying resistance free current transport through the region occupied by the DW. Although theories exist that predict a negative intrinsic DW resistance, either as a result of modifications to quantum interference phenomena<sup>12</sup> or differences in spin-dependent relaxation rates,<sup>13</sup> this result is many orders of magni-

tude greater than any negative DW resistivity previously reported in a metal.<sup>1</sup>

In this work we demonstrate the existence of a sizeable *extrinsic* contribution to the negative DW resistance measured using the experimental configuration employed in Ref. [11]. This anisotropic magnetoresistance (AMR) effect arises from the circulating currents induced by the abrupt change in the off-diagonal resistivity at 90° DW, and persists even after the resistance is averaged across the sample. An analytic expression is derived for the simplest DW orientation, supplemented by numerical results for the more general case, which also allow us to simulate the experiments where a current-driven DW is moved through a microdevice.

We consider the current flow within an infinitely long thin conducting sample with rectangular cross section, width  $w$ , thickness  $t$ . The sample lies parallel to the  $xy$  plane with the long edge parallel to the  $x$  axis (Fig. 1). A dc electrical current  $I$  flows through the sample. Ideal probes are attached and measure the potential at points on either side of the sample separated by a distance  $l$ .

The current density  $\mathbf{J}(x, y)$  is assumed to be uniform as  $x \rightarrow \pm\infty$ , and no current flows through the sides of the device:

$$\mathbf{J}(\pm\infty, y) = (I/wt, 0) = (j, 0) \quad (1a)$$

$$J_y(x, 0) = J_y(x, w) = 0. \quad (1b)$$

Within the sample,  $\mathbf{J}$  is found by satisfying current continuity and the steady state Maxwell equation, with the

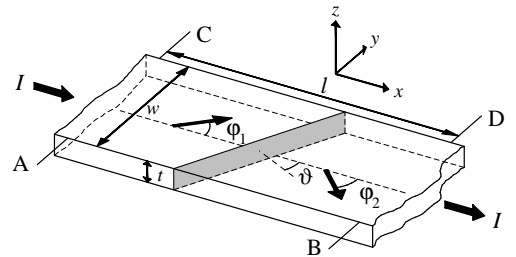


FIG. 1: The geometry considered in this work. A domain wall inclined at an angle  $\vartheta$  separates regions in which the in-plane magnetisation lies at angles  $\varphi_1$  and  $\varphi_2$ . Potential measurements are made using probes A, B, C and D.

electric field  $\mathbf{E}$  and current density related via Ohm's law

$$\nabla \cdot \mathbf{J} = 0 \quad (2a)$$

$$\nabla \times \mathbf{E} = 0 \quad (2b)$$

$$\mathbf{E} = \hat{\rho} \mathbf{J} \quad (2c)$$

with  $\hat{\rho}$  a spatially varying resistivity tensor. With in-plane magnetised (Ga,Mn)As epilayers, the resistivity in directions parallel ( $\rho_{\parallel}$ ) and perpendicular ( $\rho_{\perp}$ ) to the magnetisation differ<sup>14</sup> with  $\rho_{\parallel} < \rho_{\perp}$ . If  $\varphi$  is the magnetisation direction in a given domain (Fig. 1), the corresponding cartesian tensor is

$$\begin{aligned} \hat{\rho} &= R_{\varphi}^{-1} \begin{pmatrix} \rho_{\parallel} & 0 \\ 0 & \rho_{\perp} \end{pmatrix} R_{\varphi} \\ &= \bar{\rho} \begin{pmatrix} 1 + \frac{\beta}{2} \cos 2\varphi & \frac{\beta}{2} \sin 2\varphi \\ \frac{\beta}{2} \sin 2\varphi & 1 - \frac{\beta}{2} \cos 2\varphi \end{pmatrix} \end{aligned} \quad (3)$$

where  $\bar{\rho} = (\rho_{\perp} + \rho_{\parallel})/2$ ,  $\beta = (\rho_{\parallel} - \rho_{\perp})/\bar{\rho}$ . With cubic anisotropy, domain walls divide regions which have magnetisation directions differing by  $90^\circ$ , but in the experiments recently reported this is modified by a weak in-plane uniaxial anisotropy. We denote by  $\vartheta$  the angle which the normal to the wall ( $\hat{\mathbf{n}}_{\text{DW}}$ ) makes with respect to the  $x$  axis. Fig. 1 shows the geometry in the case of a single domain wall within the device.

At the wall itself, the boundary conditions are continuity in the normal component of the current and in the tangential component of the electric field:

$$\mathbf{J} \perp \hat{\mathbf{n}}_{\text{DW}} = J_x \cos \vartheta + J_y \sin \vartheta \quad (4a)$$

$$\begin{aligned} \mathbf{E} \parallel \hat{\mathbf{n}}_{\text{DW}} &= -E_x \sin \vartheta + E_y \cos \vartheta \\ &= -(\varrho_{xx} J_x + \varrho_{xy} J_y) \sin \vartheta \\ &\quad + (\varrho_{yx} J_x + \varrho_{yy} J_y) \cos \vartheta. \end{aligned} \quad (4b)$$

Matching (4b) when the resistivity tensor elements are different on either side of the DW is not possible with a uniform current  $\mathbf{J} = (j, 0)$ ; the DW induces circulating currents and it is these that give rise to an AMR contribution to the resistance across the wall.

To see this, we first consider the case where the device channel contains a DW in the  $yz$  plane ( $\vartheta = 0$ ) at  $x = x_0$ , separating regions in which the in-plane magnetisation is at an angle  $\varphi_1$  in region 1 and  $\varphi_2$  in region 2. The average of the longitudinal resistances measured along opposite sides of the device, used in Ref. [11] to eliminate contributions from the planar Hall effect, can be expressed in terms of a difference in voltages at either end of the device channel:

$$\begin{aligned} -I\langle R \rangle &= (V_B - V_A)/2 + (V_D - V_C)/2 \\ &= (V_B + V_D)/2 - (V_A + V_C)/2. \end{aligned} \quad (5)$$

(The minus sign is because the potential *falls* along the direction of positive current flow.) We take the length  $l$  (and  $x_0$ ) to be large enough so that the static eddy currents induced by the DW are fully contained within

the area of the device defined by the 4 probes, and then the current has its asymptotic value at both  $x = 0$  and  $x = l$ . This means that the electric field in the  $y$ -direction is constant both between C and A,  $E_y(0, y) = \rho_{yx}^1 j$ , and D and B,  $E_y(l, y) = \rho_{yx}^2 j$ , and the voltage changes linearly between points C and A, and between D and B. The voltage averages in (5) can then be re-expressed as integrals of the voltage *across* the device, e.g.

$$(V_B + V_D)/2 = \frac{1}{w} \int_0^w V(l, y) dy, \quad (6)$$

and the two terms in (5) then can be combined using  $V(l, y) - V(0, y) = -\int_0^l E_x(x, y) dx$  to give  $\langle R \rangle$  in terms of an integral of the electric field over the area of the device between the probes:

$$I\langle R \rangle = \frac{1}{w} \int_{x=0}^l \int_{y=0}^w E_x(x, y) dx dy. \quad (7)$$

Splitting the integral into separate contributions from the two domains within each of which the resistivity tensor is constant, and using the following results

$$\int_0^w J_x(x, y) dy = jw, \quad \int_0^l J_y(x, y) dx = 0 \quad (8)$$

that are found by integrating the continuity equation over regions  $\Omega = \{(x', y) \in \mathbb{R}^2 \mid 0 \leq x' \leq x, 0 \leq y \leq w\}$  and  $\Omega = \{(x, y') \in \mathbb{R}^2 \mid 0 \leq x \leq l, 0 \leq y' \leq y\}$  respectively, yields

$$\begin{aligned} \langle R \rangle &= \frac{1}{wt} [\rho_{xx}^1 x_0 + \rho_{xx}^2 (l - x_0)] \\ &\quad + \frac{1}{jw^2 t} (\rho_{xy}^1 - \rho_{xy}^2) \int_{x=0}^{x_0} \int_{y=0}^w J_y(x, y) dx dy. \end{aligned} \quad (9)$$

The first term describes a resistance that linearly interpolates between the asymptotic resistances of the channel in the two uniform magnetisation states. In Ref. [11] differences between measured resistance values and this linear interpolation have been interpreted as originating from an intrinsic DW resistivity. However, the final term in (9), which henceforth we denote  $R_{\text{AMR}}$ , is a new contribution that we find, which results directly from the discontinuity in the resistivity at the DW and which is proportional to the total parallel current induced on either side of the DW.

To obtain an estimate for the value of this additional contribution to the DW resistance, we consider the case where  $\varphi_1 = -\varphi_2 = \varphi$  which applies when the hard axis is perfectly aligned along the device channel. Then the diagonal components of the resistivity tensors are continuous across the DW, and the off-diagonal components change sign. For small  $\beta$  the longitudinal current component  $J_x$  will be dominated by the uniform background current  $j$ , except within a distance  $\sim \beta w$  of the sides of the device near the DW where the current perturbation is concentrated. Neglecting this edge correction, it then

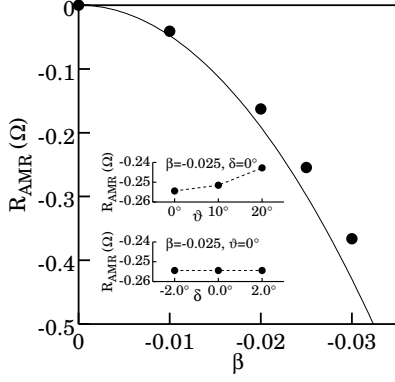


FIG. 2: Calculated AMR contribution to the resistance across a DW for different values of the anisotropy  $\beta$ . Symbols, numerically calculated values; solid line, values using Eqn. (11). A film thickness  $t = 100$  nm, resistivity  $\bar{\rho} = 3 \times 10^{-4}$   $\Omega\text{m}$ , misalignment  $\delta = 0^\circ$ , DW angle  $\vartheta = 0^\circ$  and magnetisation angle  $\varphi = 45^\circ$  have been used. Insets: the effect of varying the DW angle  $\vartheta$  and misalignment  $\delta$ .

follows from Eqn. (4) that immediately on either side of the DW

$$J_y(x_0 \pm 0^+, y) \simeq \pm \frac{j\beta}{2} \sin 2\varphi. \quad (10)$$

Ignoring anisotropy, the slowest decaying current perturbations decay like<sup>15</sup>  $\exp -\pi|x|/w$  and by assuming that  $J_y$  decays like this from the interface value (10) we can evaluate the integral in (9) to get for the AMR contribution to the average longitudinal resistance

$$R_{\text{AMR}} = -R_{\square} \frac{\beta^2}{2\pi} \sin^2 2\varphi \quad (11)$$

where  $R_{\square} = \bar{\rho}/t$  is the sheet resistance. This result shows how the circulating currents give rise to a negative contribution to the resistance across the DW.

We have also performed numerical studies of the current distributions and resulting fields and voltages in the presence of DWs. The numerical solution is not restricted to the specific configuration that was assumed in deriving the analytic estimate for  $R_{\text{AMR}}$ , so as well as enabling an assessment of the accuracy of this expression obtained we are also able to include the effects of misalignment of the hard axis with respect to the device channel, and the angle of the domain wall. Some results are given in Fig. 2. The solution is obtained by introducing a stream function  $\psi(x, y)$  that is related to the current density via  $\mathbf{J} = (\partial\psi/\partial y, -\partial\psi/\partial x)$ , thereby ensuring that current continuity Eqn. (2a) is satisfied. Combining Eqns (2b) and (2c) then results in a non-separable elliptic partial differential equation<sup>16</sup> that we solve for  $\psi$  via the multigrid relaxation method.

In Fig. 3a we show typical results from our numerical studies, displaying the variation in the longitudinal resistance as a DW inclined at an angle  $\vartheta = 20^\circ$  passes along a device channel of width  $w = 30\mu\text{m}$  and with voltage

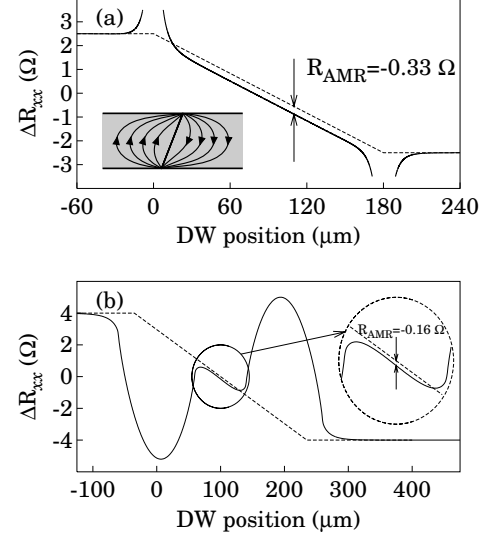


FIG. 3: (a) Variation in average resistance along the sides of the device channel (between  $x = 0$  and  $x = 180 \mu\text{m}$ ) as a function of the position of the DW. The aspect ratio is  $l/w = 6$  and the DW inclined at  $\vartheta = 20^\circ$ . See the text for the other parameters used. The inset shows the induced current flow. (b) Similar to (a) but for different material parameters (see text) and dimensions: the resistance is measured between  $x = 0$  and  $x = 200 \mu\text{m}$ ,  $l/w = 2$  and  $\vartheta = 50^\circ$ .

probes separated by  $l = 180\mu\text{m}$ . The average resistance of the two uniform magnetisation states has been subtracted:  $\Delta R_{xx} = \langle R \rangle - (\varrho_{xx}^1 + \varrho_{xx}^2)l/(2wt)$ . A general linear variation in the resistance is seen, except when the probes are within the range of the circulation currents induced by the DW; these cause a rapid variation over a distance  $\sim w \tan \vartheta + 2w/\pi$  as expected from geometrical considerations and the discussion following Eq. (10). Furthermore, we see that the calculated resistance lies *below* a straight line interpolation performed between the two asymptotic channel resistances of the two magnetisation states. In this calculation we use values that correspond as best as possible to the system reported in Fig. 4 of Ref. [11]: film resistivity  $\bar{\rho} = 3 \times 10^{-4}$   $\Omega\text{m}$ , thickness  $t = 100$  nm, and anisotropy<sup>18</sup>  $\beta = -0.03$ . The magnetisation orientations within the two domains are taken to be  $\phi_1 = \delta + \phi$ ,  $\phi_2 = \delta - \phi$  where  $\phi = 37^\circ$  due to uniaxial anisotropy<sup>14,17</sup> and the misalignment  $\delta = -0.28^\circ$  (the difference between the asymptotic resistances,

$$(\varrho_{xx}^2 - \varrho_{xx}^1) \frac{l}{wt} = \frac{\bar{\rho} \beta l}{wt} \sin 2\phi \sin 2\delta, \quad (12)$$

is then  $5 \Omega$  as found in Ref. [11]). Using these values, numerically we find the resistance is lowered by  $0.33 \Omega$  as a result of the eddy currents induced by the DW.

In Fig. 2 we compare numerical values for  $R_{\text{AMR}}$  found in a number of similar calculations to that just described, with those obtained using Eqn. (11). The numerical results also display the  $\beta^2$  dependence and, as expected

given the approximations made in estimating the current integral, our analytic expression overestimates the actual resistance, we find by approximately 15% when  $\vartheta = 0$ . This value of  $R_{\text{AMR}}$  is further reduced at DWs inclined relative to the current direction, but is relatively insensitive to the misalignment angle (insets in Fig. 2). Thus Eqn. (11) has some value in estimating the AMR contribution to the DW resistance, but numerical calculations are required for accurate estimates.

In Fig. 3b we show the calculated longitudinal resistance for a second case, with parameters chosen to correspond to the device reported in Fig. 1 in Ref. [11]. This was the initial device studied experimentally, in which the misalignment of the hard axis with the device channel is greater. We use  $\bar{\varrho} = 4 \times 10^{-4} \Omega\text{m}$ ,  $t = 150 \text{ nm}$ ,  $\beta = -0.03$ , with the channel width  $w = 100 \mu\text{m}$  and voltage probes separated by  $200 \mu\text{m}$ . Also,  $\phi = -37^\circ$ ,  $\delta = 1.5^\circ$ . The greater structure exhibited by  $\Delta R_{xx}$  in this case is due to a larger DW inclination ( $\vartheta = 50^\circ$ ) and the smaller aspect ratio  $l/w$  of the device, and results in a linear variation over only a short range of DW positions midway between the voltage probes. The precise results are rather sensitive to the value of  $\vartheta$ . However, generally we find that in the linear region the large spatial extent of the eddy currents still affects the slope of the resistance curve, which no longer coincides with a linear interpolation of the asymptotic resistances between the probe positions. The dashed line in Fig. 3b which is parallel to the linear section of the resistance curve connects points some 30% further apart than the probes. The calculated resistance is again lowered due to the AMR, but the difference of  $-0.16 \Omega$  is smaller than the value ( $-0.18 \Omega$ ) found if the distance between the voltage probes is increased so as to fully contain the eddy currents.

The magnetisation profile *within* the wall can also give rise to a negative AMR. However, the contribu-

tion we describe above dominates here. Assuming a  $90^\circ$  Néel like wall with magnetisation rotating like  $\phi(x) = -(1/2) \tan^{-1} \sinh x/\lambda$ , where  $\pi\lambda$  is the wall width, gives a contribution to leading order of  $\lambda/(-2\beta w)R_{\text{AMR}}$ , or just a few percent of the contribution from the circulation currents. Other wall profiles in which the spin rotates out of the plane lead to the same conclusion. Only if the DWs in this system were  $180^\circ$  walls would the in-wall contribution be significant, since then the circulation current contribution (11) vanishes.

Comparing with experiment, the DW resistances reported in [11] for the devices modelled in Figs 3a and 3b are  $-1.0 \pm 0.2 \Omega$  and  $-0.44 \pm 0.5 \Omega$  respectively; a third set of devices similar to that of Fig. 3a but with  $w = 60 \mu\text{m}$  gave  $-0.3 \pm 0.2 \Omega$ . The corresponding  $R_{\text{AMR}}$  values we find are  $-0.33 \Omega$ ,  $-0.16 \Omega$  and  $-0.33 \Omega$ . The previously neglected AMR contributions to the resistance across the DW make a major contribution to, and can largely explain, the negative values observed, with the exception of one set of devices where a true negative intrinsic DW resistance may indeed have been observed. Clearly further experiments are required to clarify the situation, before attempts to quantitatively account for the DW resistance<sup>19</sup> can be properly assessed. For these, devices with a large aspect ratio  $l/w$ , and containing DWs orientated normal to the device channel, are clearly desirable.

To summarise, we have identified a significant anisotropic magnetoresistance contribution to the negative domain wall resistivities recently observed in microdevices fabricated from (Ga,Mn)As epilayers. We derive an analytic estimate of the magnitude of this contribution, and report calculations of the channel resistance as a DW is moved through the device which provide a good description of the experiments.

This work was supported by the Leverhulme Trust, through Grant No. F/00 351 F.

- 
- <sup>1</sup> For a review, see C.H. Marrows, Adv. in Phys. **54**, 585 (2005).  
<sup>2</sup> D. Ravelosona *et al.*, Phys. Rev. B **59**, 4322 (1999); M. Viret *et al.*, Phys. Rev. Lett. **85**, 3962 (2000); A.D. Kent, J. Yu, U. Rüdiger and S.S.P. Parkin, J. Phys.: Condens. Matter **13**, R461 (2001); R. Danneau *et al.*, Phys. Rev. Lett. **88**, 157201 (2002); C.H. Marrows and B.C. Dalton, Phys. Rev. Lett. **92**, 097206 (2004); A. Aziz *et al.*, Phys. Rev. Lett. **97**, 206602 (2006).  
<sup>3</sup> M. Viret *et al.*, Phys. Rev. B **53**, 8464 (1996).  
<sup>4</sup> P.M. Levy, and S. Zhang, Phys. Rev. Lett. **79**, 5110 (1997).  
<sup>5</sup> N. García, M. Munõz, and Y.-W. Zhao, Phys. Rev. Lett. **82**, 2923 (1999); P. Bruno, Phys. Rev. Lett. **83**, 2425 (1999).  
<sup>6</sup> G. Tatara and H. Kohno, Phys. Rev. Lett. **92**, 086601 (2004).  
<sup>7</sup> M. Yamanouchi *et al.*, Phys. Rev. Lett. **96**, 096601 (2006).  
<sup>8</sup> G. Vignale and M.E. Flatté, Phys. Rev. Lett. **89**, 098302 (2002).  
<sup>9</sup> C. Rüster *et al.*, Phys. Rev. Lett. **91**, 216602 (2003).

- <sup>10</sup> D. Chiba *et al.*, Phys. Rev. Lett. **96**, 096602 (2006).  
<sup>11</sup> H.X. Tang *et al.*, Nature (London) **431**, 52 (2004).  
<sup>12</sup> G. Tatara and H. Fukuyama, Phys. Rev. Lett. **78**, 3773 (1997); Y. Lyanda-Geller, I.L. Aleiner and P.M. Goldbart, Phys. Rev. Lett. **81**, 3215 (1998).  
<sup>13</sup> R.P. van Gorkom, A. Brataas and G.E.W. Bauer, Phys. Rev. Lett. **83**, 4401 (1999).  
<sup>14</sup> H.X. Tang *et al.*, Phys. Rev. Lett. **90**, 107201 (2003).  
<sup>15</sup> R.T. Bate, J.C. Bell, and A.C. Beer, J. Appl. Phys. **32**, 806 (1961).  
<sup>16</sup> A similar approach was used in [17] but the series solution then obtained does not satisfy the original equation.  
<sup>17</sup> H. Tang and M.L. Roukes, Phys. Rev. B, **70**, 205213 (2004).  
<sup>18</sup> We determine  $\beta$  from the quoted values of the planar Hall resistance  $R_{xy}$ , using  $\beta = -2R_{xy}t/\bar{\varrho} \sin 2\phi$ .  
<sup>19</sup> R. Oszwaldowski, J.A. Majewski, and T. Dietl, Phys. Rev. B **74**, 153310 (2006); A.K. Nguyen, R.V. Shchelushkin, and A. Brataas, Phys. Rev. Lett. **97**, 136603 (2006).